Magyarhoni Földtani Társulat
Földtani Közlöny
Hungarian Geological Society

152/3, 201–212., Budapest, 2022

DOI: 10.23928/foldt.kozl.2022.152.3.201

Study on andorite-series minerals from the Meleg Hill, Velence Mts., Hungary

Papp, Richard Z.[1*], Topa, Boglárka A.[2], Zajzon, Norbert[3]

[1]University of Miskolc, Institute of Mineralogy and Geology; askprz@uni-miskolc.hu
[2]University of Miskolc, Institute of Mineralogy and Geology; boglarka.topa@uni-miskolc.hu
[3]University of Miskolc, Institute of Mineralogy and Geology; nzajzon@uni-miskolc.hu
*Correspondence: askprz@uni-miskolc.hu

Az andoritsor ásványainak vizsgálata a velencei-hegységi Meleg-hegy területéről

Összefoglalás

A Meleg-hegy (Velencei-hegység) paleogén korú hidrotermás breccsájának északkeleti, antimonitban gazdag részéből származó breccsaminták elektronmikroszondás vizsgálata során két új, a területről eddig nem ismert ásványfajt találtunk. Az ásványok a lillianit homológ sorba tartozó andoritsor tagjainak bizonyultak. Kémiai összetételük és az andorit helyettesítési százalékuk (L%) alapján andorit VI-ként és roscsinitként azonosíthatóak.

Az andorit VI 6 kénatomra normált képlete az átlagos kémiai összetétel alapján $Ag_{1.06}Cu_{0.04}Pb_{0.80}Sb_{2.49}Bi_{0.22}As_{0.3}S_6$ (L% = 102,65 – 109,84), a roscsinit 96 kénatomra normált képlete $Ag_{17.23}Cu_{0.53}Pb_{10.4}Hg_{0.04}Zn_{0.04}Fe_{0.02}Sb_{39.73}Bi_{5.52}As_{5.98}S_{96}$ (L% = 119,52 – 123,48). Eredményeink arra utalnak, hogy a korábban alkalmazott összehasonlító $(Ag_2S + Cu_2S)$–$(Sb_2S_3 + Bi_2S_3 + As_2S_3)$ – (PbS + HgS + FeS + ZnS + CdS) háromszögdiagram nem elégséges az andoritsor ásványainak pontos elkülönítéséhez az Me^+, Me^{2+} és Me^{3+} kationok esetében megjelenő változó elemhelyettesítések miatt. Ez alapján kijelenthető, hogy az andorit helyettesítési százalék (L%) és az andorit homológ érték (N) kiszámítása minden esetben elengedhetetlen az andoritásványok fajszintű meghatározásához.

Tárgyszavak: andorit VI; kémiai változatosság; roscsinit; szulfosó; Velencei Gránit Formáció

Abstract

During the last decades, different sulphosalts were observed in several samples that were investigated from the Meleg hill, Velence Mts. The investigated sample of this study was collected from the less studied north-eastern, stibnite-rich part of the hydrothermal breccia at the Meleg Hill. Based on the results of electron microprobe analysis, we found that the sample contained two sulphosalt minerals of the andorite series that have not been described from Hungary before. The andorite series is a subgroup of the lillianite homologous series. The individual minerals, andorite VI and roshchinite, within the andorite series were identified on the basis of their chemical composition and the andorite substitution percentage (L%).

Andorite VI has $Ag_{1.06}Cu_{0.04}Pb_{0.80}Sb_{2.49}Bi_{0.22}As_{0.3}S_6$ average chemical formula (normalized to six sulphur atoms) and L% = 102.65–109.84, whereas roshchinite has $Ag_{17.23}Cu_{0.53}Pb_{10.4}Hg_{0.04}Zn_{0.04}Fe_{0.02}Sb_{39.73}Bi_{5.52}As_{5.98}S_{96}$ average chemical formula (normalized to 96 sulphur atoms) and L% = 119.52–123.48. Our results suggest that the formerly used comparative ternary diagrams of the system $(Ag_2S + Cu_2S)$–$(Sb_2S_3 + Bi_2S_3 + As_2S_3)$–(PbS + HgS + FeS + ZnS + CdS) is not adequate to differentiate the andorite-series minerals from each other, due to the highly variable element substitution of Me^+, Me^{2+} and Me^{3+} cations. The andorite substitution percentage (L%) and the andorite homologue order value (N) are always necessary to calculate to distinguish the mineral species.

Keywords: andorite VI; chemical variability; roshchinite; sulphosalt; Velence Granite Formation

Introduction

In the last few years, numerous samples were collected from the southern part of Meleg Hill, Velence Mountains, Hungary (*Figure 1*). The sampling aimed to collect minerals for different Hungarian mineral collections (e.g., Herman Ottó Museum in Miskolc, Hungary) and for the CriticEl project between 2012–2014 to assess potential mineral deposits in Hungary. They were studied with scanning electron microscopy (SEM) and electron microprobe analysis (EPMA), but only one of them contained andorite-series minerals.

Andorite-series minerals (*Table I*) usually crystallize in low-temperature polymetallic hydrothermal veins in a stibnite, sphalerite, quartz, pyrite, tetrahedrite, pyrargyrite comprising the paragenesis in the final stage of mineralization after the precipitation of stibnite (OZDÍN & SEJKORA 2009, PRŠEK et al. 2009). Their significance in ore-forming processes is currently unknown due to their complex structure and difficulties in their identification.

In some earlier studies, andorite VI may have been referred to as senandorite, andorite IV quatrandorite and the copper-rich variety of andorite VI, nakaséite.

The aim of this work was to identify these minerals and understand their genetic significance. These newly found minerals, andorite VI and roshchinite, have not been described in detail and nor mentioned previously from Hungary due to the very detailed chemical measurements which are required to distinguish them from each other. The average chemical composition of these minerals is similar (*Table I*); therefore, special parameters, such as andorite homologue order value [N] and substitution percentage [L%], are used for their distinction. These values can be calculated from the chemical composition. The chemical composition also causes problems during the measurements, because the PbM and the SK (and the HgM) lines overlap on the energy-dispersive spectrum, therefore the EDX systems are not suitable for quantification of these elements. Moreover, the minute size (mainly 0.5–15 μm and only occasionally 30–50 μm) of the grains and the chemical inhomogeneity also cause difficulties during the measurements.

Geological setting

The Meleg Hill is situated in the Velence Mountains, in Hungary. The Velence Mts., in turn, is situated on the Southern margin of the Transdanubian Mountain Range (TMR) along the Periadriatic–Balaton Line (PABL).

The TMR was originally situated between the Eastern and Southern Alps and in the late Paleogene to Early Neogene it moved out from the Alpine collision zone. This process was also accompanied by the right-lateral displacement of the Velence Mountains to its current position (BALLA 1985, KÁZMÉR & KOVÁCS 1985, CSONTOS & VÖRÖS 2004, BENKÓ et al. 2014).

The Velence Mountains can be divided into two main igneous rock units. The intrusion of the western part consists of the rocks of the Permian Velence Granite Formation, meanwhile, the eastern part is built up by the rocks of the Oligocene Nadap Andesite Formation (Palaeogene Volcanic Unit – PVU). Both igneous units were intruded into the rocks of the Ordovician to Devonian Lovas Slate Formation.

From geochemical and geochronological points of view, the granite of the Velence Mts. is comparable to other A-type granites along the PABL formed after the Variscan orogeny (BUDA et al. 2004, UHER & BROSKA 1994, GYALOG & HORVÁTH 2004). According to studies of BUDA (1993), MOLNÁR et al (1995) and Molnár (1997), this granite was formed at a pressure of 2 kbar and in the temperature range of 550–690 °C.

In the late stage of the crystallization of the granite, aplite and granite porphyry dykes were formed by the intrusion of the residual melt. These dykes are oriented northeast-southwest throughout the whole granite body (JANTSKY 1957, HORVÁTH et al. 2004)

The PVU is situated in the eastern part of the Velence Mountains, east from the Nadap Line. The hydrothermally altered andesitic stratovolcanic sequence is underlain by a diorite intrusion.

The area of the Velence Mountains was affected by several different hydrothermal alteration events during the Permian, the Triassic and the Paleogene periods (MOLNÁR et al. 1995; MOLNÁR 1996, 1997, 2004; BENKÓ et al. 2008, 2012, 2014; TÓTH 2016; KOVÁCS et al. 2019, 2020). The Permian, Triassic and Paleogene hydrothermal events distinguished by characteristic clay mineral and fluid inclusion assemblages are summarized in *Table II*.

In the hydrothermal breccia of Meleg Hill, two different element enrichments can be observed: (1) enargite-bearing siliceous alteration with different fahlores are characteristic in the north-western part and (2) antimony-rich minerals including stibnite, (Ag)-Sb-Pb sulphosalts and antimony

→ **Figure 1.** A: Location of Meleg Hill, Velence Mountains; B: Geological map of the Velence Mountains (GYALOG 2005a, 2005b); C: Schematic geological map of Meleg Hill after TÓTH (2016) and the occurrence of the andorite-series minerals

Legend: 1 = artificial fill; 2–17 = Pleistocene and Holocene formations; 18 = Pannonian Tihany Formation; 19–21 = Pannonian sediments; 22 = Oligocene Pázmánd Metasomatite Member of the Nadap Andesite Formation; 23 = Oligocene Sorompóvölgy Andesite Member of the Nadap Andesite Formation; 24 = Upper Cretaceous Budakeszi Picrite Formation; 25 = Cretaceous quartz vein; 26 = Lower Permian Velence Granite Formation; 27 = Lower Permian Pákozd Granite Porphyry Member of the Velence Granite Formation; 28 = Lower Permian Kisfalud Microgranite Member of the Velence Granite Formation; 29 = Silurian–Devonian Bencehegy Microgabbro Formation; 30 = Ordovician–Devonian Lovas Slate Formation; 31 = Hydrothermal breccia at the Meleg Hill area; 32 = Granite porphyry in the Velence Granite Formation; 33 = Aplite and microgranite in the Velence Granite Formation; 34 = Nadap Line; 35 = Nadap–Lovasberény road; 36 = Enargite-bearing siliceous alteration at Meleg Hill; 37 = Stibnite rich hydrothermal breccia at Meleg Hill; 38 = Locality of the investigated sample; Abbreviation: Szfv. = Székesfehérvár

→ ***1. ábra.*** *A: A Velencei-hegység elhelyezkedése; B: A Velencei-hegység és északi előterének földtani térképe (GYALOG 2005a, b alapján). C: A Meleg-hegy sematikus geológiai térképe TÓTH (2016) alapján és az andoritsor ásványainak előfordulása*

Jelmagyarázat: 1 = mesterséges feltöltés; 2–17 = pleisztocén és holocén formációk; 18 = pannóniai Tihanyi Formáció; 19–21 = pannóniai üledékek; 22 = középső–első eocén Nadapi Andezit Formáció Pázmándi Metaszomatit Tagozata; 23 = középső–felső eocén Nadapi Andezit Formáció Sorompóvölgyi Andezit Tagozata; 24 = felső kréta Budakeszi Pikrit Formáció; 25 = kréta kvarctelér; 26 = alsó perm Velencei Gránit Formáció; 27 = alsó perm Velencei Gránit Formáció Pákozdi Gránitporfír Tagozata; 28 = alsó perm Velencei Gránit Formáció Kisfaludi Mikrogránit Tagozata; 29 = szilur–devon Bencehegyi Mikrogabbró Formáció; 30 = ordovícium–devon Lovasi Agyagpala Formáció; Szfv.-i blokk = Székesfehérvári blokk

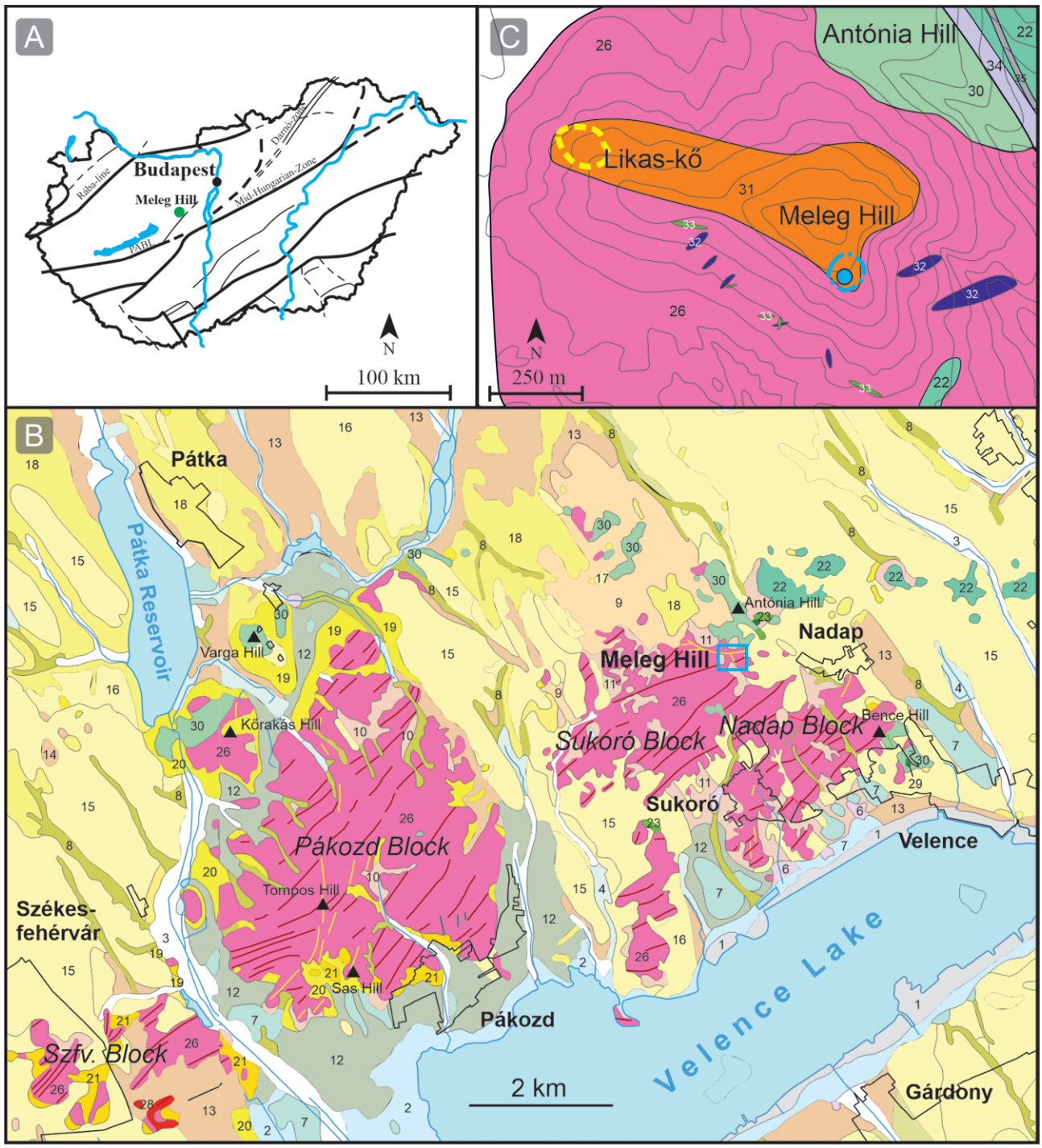
A
Budapest
Meleg Hill
Rába-line
PABL
Mid-Hungarian-Zone
Darnó-zone
N
100 km
C
Antónia Hill
Likas-kő
Meleg Hill
N
250 m
B
Pátka
Pátka Reservoir
Varga Hill
Kőrakás Hill
Pákozd Block
Tompos Hill
Sas Hill
Szfv. Block
Székes-
fehérvár
Pákozd
Meleg Hill
Antónia Hill
Nadap
Sukoró Block
Nadap Block
Bence Hill
Sukoró
Velence
Velence Lake
Gárdony
2 km

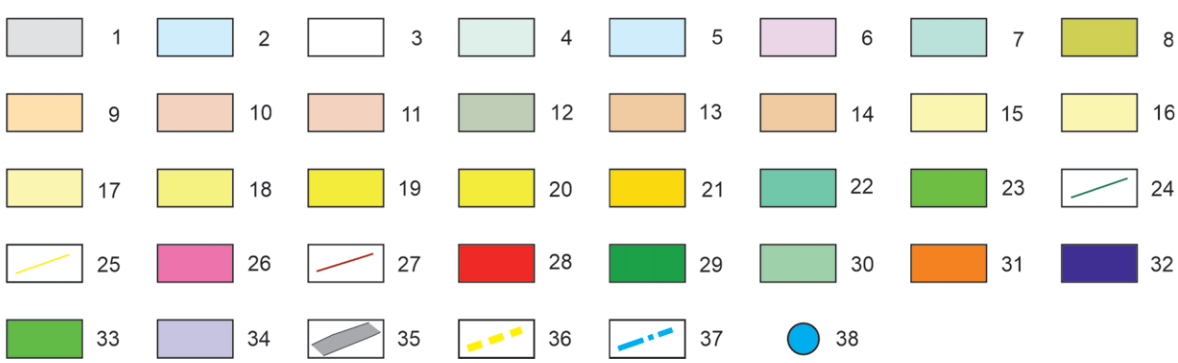
1 2 3 4 5 6 7 8
9 10 11 12 13 14 15 16
17 18 19 20 21 22 23 24
25 26 27 28 29 30 31 32
33 34 35 36 37 38

Table I. Minerals of the andorite-series with their chemical composition, space group, substitution percentage (L%) and andorite homologue order value (N) (MOËLO et al. 2013, PAŽOUT 2017)

I. táblázat. *Az andoritsor ásványainak kémiai összetétele, tércsoportjuk, helyettesítési százalékuk (L%), valamint andorithomológ értékük (N) (MOËLO et al. 2008, PAŽOUT 2017)*

Name	Chemical composition	Space group	L%	N
uchucchacuaite	$Pb_3MnAgSb_5S_{12}$	*Pmmm*	And_{50}	4
fizélyite	$Ag_5Pb_{14}Sb_{21}S_{48}$	$P2_1/n$	$And_{62.5}$	4
ramdohrite	$(Cd,Mn,Fe)Ag_{5.5}Pb_{12}Sb_{21.5}S_{48}$	$P2_1/n$	$And_{68.75}$	4
andorite IV	$Ag_{15}Pb_{18}Sb_{47}S_{96}$	*P2*	$And_{93.75}$	4
andorite VI	$AgPbSb_3S_6$	$Pmn2_1$	And_{100}	4
arsenquatrandorite	$Pb_{12.8}Ag_{17.6}Sb_{38.08}As_{11.52}S_{96}$	$P2_1/b$	And_{110}	4
roshchinite	$Pb_{10}Ag_{19}Sb_{51}S_{96}$	*Pnma*	And_{115}	4
oscarkempffite	$Pb_4Ag_{10}Sb_{17}Bi_9S_{48}$	*Pnca*	And_{124}	4
clino-oscarkempffite	$Pb_6Ag_{15}Sb_{21}Bi_{18}S_{72}$	$P2_1/b$	And_{125}	4
jasrouxite	$Pb_4Ag_{16}Sb_{24}As_{16}S_{72}$	*P-1*	$And_{136.5}$	4

oxides are dominant in the southern part (*Figure 1/C*). The antimony oxides were produced during the alteration processes of the original Sb-rich ore. The investigated andorite-series mineral-bearing sample was collected from this latter zone of the hydrothermal breccia.

Analytical methods and sample preparation

During sample preparation, polished surface mounts were made. The samples were vacuum impregnated in Araldite epoxy resin. Once solidified, they were cut and their surface was ground under dry condition on SiC abrasive paper and polished with diamond paste (6 µm, 3 µm, 1 µm, 1/4 µm) under wet conditions. Alcohol-based lubricant was used to avoid any oxidation of the sample surface during the process.

The analytical measurements (SEM and EMPA) were performed at the Department of Mineralogy and Geology and at the 3D Lab at the University of Miskolc. Further EMPA analyses were made at the Department of Electron Microanalysis, Geological Institute of Dionýz Štúr in Bratislava, Slovakia.

Electron microprobe measurements were performed on a JEOL JXA-8600 Superprobe with upgraded SAMX software, 20 kV acceleration voltage and 20 nA beam current (Miskolc) and with a Cameca SX-100 microprobe with 25 kV acceleration voltage and 10 nA beam current (Bratislava). *Table III* contains the analyser crystal types and standards that were used during the wavelength-dispersive X-ray spectroscopic (WDX) measurements.

The SEM images were taken with a Thermo Scientific Helios G4PFIB XCe, Xe Plasma Focused Ion Beam Scanning Electron Microscope, equipped with an EDAX Team Pegasus system (Octane detector), with 15–20 kV acceleration voltage and 3.2–13 nA beam current. The acceleration voltage and the beam current were modified according to the method of use (imaging or chemical measurement).

Due to the size of the minerals examined, optical microscopy was not used for further mineral identification.

Table II. Summary of the hydrothermal events of Velence Mts. based on BENKÓ et al. (2014) and KOVÁCS et al. (2019); P = Permian, T = Triassic, Ol_1 = Lower Oligocene

II. táblázat. A Velencei-hegység hidrotermás eseményeinek összefoglalása BENKÓ et al. (2014) és KOVÁCS et al. (2019) alapján; P = perm, T = triász, Ol_1 = alsó oligocén

Formation	Total homogenization temp., Formation pressure	Age	References
quartz–molybdenite–pyrite–fahlore mineralization	220–320 °C, 1.3–2.5 kbar	P	MOLNÁR 1997
base-metal veins with fluorite	70–180 °C, 0.4–0.5 kbar, 190–245 °C, 0.4–0.5 kbar	T	BENKÓ et al. 2008, 2010, 2014; MOLNÁR 1996
diorite intrusion, andesite vulcanism		Ol_1	DARIDA-TICHY 1987, BENEDEK et al. 2004
HS-type epithermal mineralization in andesite	220–290 °C, 160–200 bar 310–380 °C, 160–200 bar	Ol_1	MOLNÁR 1996, 1997; MOLNÁR et al. 1995; BAJNÓCZI et al. 2010
hydrothermal breccia, enargite-bearing siliceous alteration	260–460 °C	Ol_1	MOLNÁR 1996, 1997; MOLNÁR et al. 1995
porphyry copper	220–570 °C, 100–280 bar	Ol_1	MOLNÁR 1996, BAJNÓCZI et al. 2010, MOLNÁR et al. 2010
quartz-barite veins, illitic alteration	150–200 °C, 30–40 bar ~220 °C, 30–40 bar	Ol_1	BENKÓ et al. 2012, KOVÁCS et al. 2020

Crystal chemical calculations in the andorite series

Andorite-series minerals are the Sb-rich members of the lillianite homologous series. The minerals of the lillianite homologous series are complex sulphides with Pb-Bi-Sb-Ag-S chemistry. The crystal structure of the lillianite series is built up from alternating layers of PbS parallel to the $(311)_{PbS}$ lattice plane. In the case of the andorite-series minerals, under- and oversubstitution can be observed by the replacement of the Pb atom in these alternating PbS layers.

For our calculations, we used the work of MAKOVICKY & KARUP-MØLLER (1977a, 1977b) and MAKOVICKY (2019) regarding the

Table III. List of analysing crystals and standards used in this study with corresponding measured elements (normal font: University of Miskolc; italic font: Geological Institute of Dionýz Štúr).

III. táblázat. *A különböző ásványok mérése során használt analizátorkristályok és sztenderdek (normál betűk: Miskolci Egyetem; dőlt betűk: Geological Institute of Dionýz Štúr)*

Element	Anal. crystal	Standard
As Lα	TAP/*TAP*	GaAs/*GaAs*
Ag Lα	PET/*LPET*	Ag/*Ag*
S Kα	PET/*LPET*	MnS_2/*CuFeS*$_2$
Cu Lα/*Kα*	TAP/*LLIF*	Cu_3Se_2/*CuFeS*$_2$
Sb Lα	PET/*LLIF*	Sb_2S_3/*Sb*
Bi Mα/*Lα*	PET/*LLIF*	Bi/*Bi*
Fe Kα	LIF/*LLIF*	FeS_2/*CuFeS*$_2$
Pb Mα	PET/*LPET*	PbS/*PbS*
Zn Lα/Kα	TAP/*LLIF*	Zn/*ZnS*
Hg Lα	LIF/*LLIF*	HgS/*HgS*

classification of the lillianite series. This classification is based on the lillianite homologue, the molar fraction and the substitution percentage of the phases.

The andorite homologue value (N) was calculated with the following equation:

$$N = -1 + 1 / (Sbi + Pbi / 2 - 1 / 2) \quad (1)$$

where Sbi = Sb / (Ag + Sb + Pb) Pbi = Pb / (Ag + Sb + Pb); Sb = Sb + Bi + As; Ag = Ag + Cu and Pb = Pb + Zn + Hg + Cd (Moëlo et al. 1984, Makovicky 2019).

The substitution percentage (L%) of the Ag-Sb end member of the andorite is equal to

$$L\% = 1 - (2Sbi - Pbi - 1) / 6 \times (Bi + Pbi / 2 - 5 / 6) \times 100 \quad (2)$$

and the substitution parameter is:

$$x = (L\% \times (N - 2)) / 20 \quad (3)$$

The equations were calculated with the chemical formula of andorite VI ($PbAgSb_3S_6$).

The andorite series comprises well-defined minerals with limited composition ranges and limited content of specific minor elements. The substitution percentages of the andorite-series minerals can be seen in *Table I*, but due to the continuous under- and oversubstitution of the specimens in nature, the substitution percentage can be described as a continuous range between the two neighbouring mineral species (Moëlo et al. 2008, Pažout 2017).

N and L values were calculated for selected members of the andorite series from different localities based on analytical data taken from earlier publications (Kostov & Minčeva-Stefanova 1981; Makocivky & Mumme 1983; Moëlo 1984; Moëlo et al. 2008; Makovicky et al. 2013, 2018) (*Table I*).

Results

The andorite-series minerals occur as 1–50 μm crystals at Meleg Hill (*Figure 2/A*) in the hydrothermal breccia. Several smaller grains have a flame-like appearance, where the edge of the crystals is fibrous (*Figure 2/B*). Larger (20–50 μm) grains are chemically inhomogeneous (*Figure 2/C*). The andorite-series minerals are enclosed in the siliceous matrix of the breccia. Several different As-Sb-Pb sulphosalts (enargite, tennantite, tetrahedrite) and sulphides (stibnite, galena, pyrite, sphalerite and chalcopyrite) are associated with the grains of the andorite-series minerals.

Due to the small grain size (less than 5 μm in diameter), not all the crystals can be measured accurately. At an accelerating voltage of 20–25 kV, the interaction volume of the penetrating electron beam can be larger than the volume of the mineral. This effect can cause incomprehensible chemical information. The same problem occurs when the width of the mineral to be examined is less than 1 μm since the diameter of the electron beam is comparable with this size. To validate the results and get the proper chemical composition of the minerals, the same crystals were analysed with two different electron microprobes. Altogether 25 different point measurements were performed on the sample to get the precise chemical composition. Based on these duplicate analyses, two different phases can be distinguished. *Table IV* and *Table V* contain the chemical compositions in wt%. The main chemical features of the phases are similar, but characteristic differences can be observed in the lead, bismuth and arsenic content. This chemical inhomogeneity on the backscattered electron images is easily recognisable.

The andorite homologue number (N) and the substitution percentage (L%) of the phases are also different. For the first mineral the average values are: N = 4.17, L% = 107.07 and for the second mineral N = 3.70, L% = 121.41 (*Table IV* and *Table V* contain the N and L% for all the measured points).

Discussion

Based on the analytical data, the andorite homologue value (N) and the substitution percentage (L%) calculations, two different types of andorite-series minerals can be distinguished in the sample with the following average compositions and values:

– andorite VI:

$$Ag_{1.06}Cu_{0.04}Pb_{0.8}Sb_{2.49}Bi_{0.22}As_{0.3}S_6$$

N = 4.17, L% = 107.07

– roshchinite:

$$Ag_{17.23}Cu_{0.53}Pb_{10.4}Hg_{0.04}Zn_{0.04}Fe_{0.02}Sb_{39.73}Bi_{5.52}As_{5.98}S_{96}$$

N = 3.70, L% = 121.41

Table VI and *Table VII* contain the chemical formulae calculated from the analytical data; normalized to six sulphur atoms for andorite VI and 96 for roshchinite, compared with the theoretical composition of the given minerals.

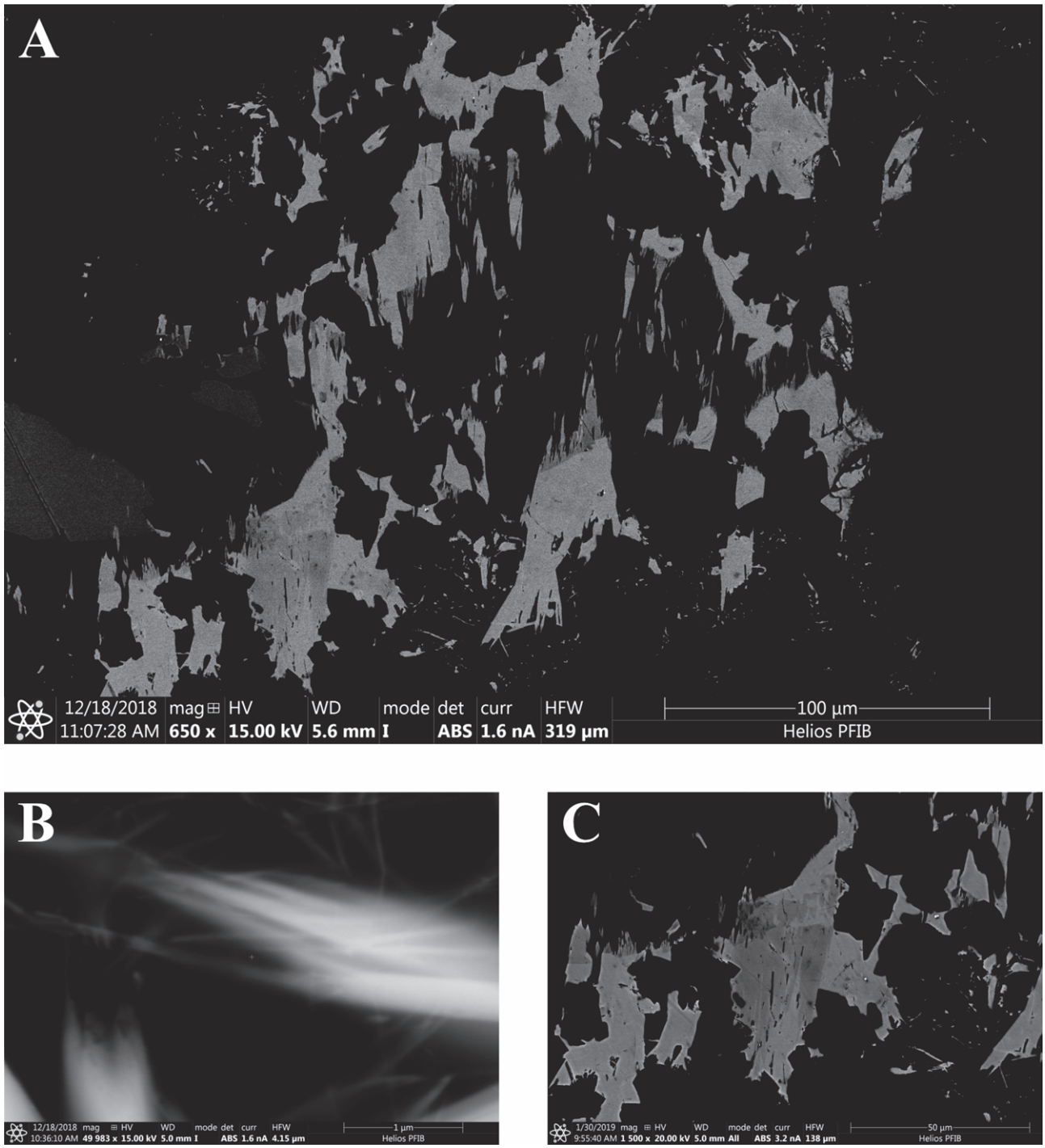

Figure 2. Backscattered electron (BSE) images of the andorite-series minerals from the Meleg Hill; A: overview image of the andorite-series crystals; B: minerals with fibrous habit; C: Different shades of grey corresponds to the different compositions within a grain in a BSE image

2. ábra. *A Meleg-hegyen azonosított andoritsor ásványainak visszaszórtelektron-képe (BSE); A: összefoglaló kép az andoritsor kristályairól; B: szálas habitusú ásványok; C: a szürke különböző árnyalatai az ásványok kémiai összetételének eltérését mutatják a BSE-felvételeken*

The theoretical homologue value for the lillianite-group minerals is N = 4, but in the case of the andorite-series, it may deviate from 4 due to the element substitution in the different sites. In the andorite VI grains from Meleg Hill the Me^{2+} cation Pb is undersubstituted and the Me^{3+} cation Sb is replaced with minor Bi and As compared to the theoretical composition ($Ag^{+}Pb^{2+}Sb^{3+}{}_3S_6$). In the roshchinite grains, the Me^{2+} and Me^{3+} cations are oversubstituted, and the Me^{+} is undersubstituted (the theoretical composition for roshchinite is $Ag^{+}{}_{19}Pb^{2+}{}_{10}Sb^{3+}{}_{51}S_{96}$). In this case, higher Bi-As replacement can be observed in the Sb position.

Based on the measured wt% of the Me^{+}, Me^{2+} and Me^{3+} cations, two different kinds of minerals can be distinguished in the Meleg Hill samples (*Figures 3–4*). The chemical com-

Table IV. Results of the electron microprobe analysis of andorite VI grains from Meleg Hill in weight percent (wt%) together with the calculated andorite homologue number (N) and substitution value (L%) (bdl = below the detection limit; No.: measurement ID)

IV. táblázat. *A meleg-hegyi andorit VI kristályok elektronmikroszondás mérési eredményei tömegszázalékban (wt%) , valamint a számított andorit-homológ értékek (N) és a helyettesítési százalékok (L%) (bdl = kimutatási határérték alatt; No.: a mérés sorszáma)*

No.	Ag	Cu	Pb	Fe	Hg	Zn	Sb	Bi	As	S	Total	N	L%
1	12.94	0.40	18.06	0.04	bdl	0.07	35.95	6.79	1.46	22.34	**98.06**	4.09	109.54
2	13.48	0.37	17.69	0.01	bdl	0.05	35.75	7.22	1.63	22.41	**98.61**	4.17	109.84
3	13.08	0.19	20.43	bdl	0.18	bdl	37.29	3.69	2.46	21.76	**99.08**	3.99	107.29
4	13.88	0.32	18.10	bdl	0.14	bdl	36.63	4.88	2.39	22.20	**98.54**	4.19	109.53
5	13.12	0.19	20.41	bdl	0.18	bdl	37.32	3.69	2.45	22.94	**100.30**	4.01	107.16
6	14.25	0.32	18.25	bdl	0.14	bdl	36.47	4.92	2.38	23.40	**100.13**	4.33	107.95
7	14.47	0.33	18.12	bdl	bdl	0.03	36.31	2.89	4.15	23.62	**99.92**	4.24	109.51
8	13.91	0.18	16.27	0.02	0.14	bdl	33.49	8.77	2.77	24.38	**99.93**	4.19	108.36
9	13.05	0.09	17.94	0.01	0.08	bdl	35.77	6.47	2.62	23.61	**99.64**	4.06	107.35
10	13.12	0.54	20.41	bdl	bdl	bdl	33.94	5.10	2.78	23.09	**98.98**	4.41	102.65
11	12.78	0.53	20.41	bdl	0.26	bdl	34.57	5.14	2.68	23.22	**99.59**	4.25	103.65
12	12.90	0.30	20.09	bdl	bdl	bdl	35.46	4.96	2.68	23.57	**99.96**	4.05	106.94
13	12.78	0.29	20.71	0.04	0.11	bdl	35.31	4.29	3.02	22.95	**99.50**	4.05	105.76
14	13.23	0.39	20.50	0.01	bdl	bdl	36.05	4.17	3.13	23.29	**100.77**	4.11	106.46
15	13.93	0.17	20.61	0.02	bdl	bdl	34.65	5.71	2.69	22.02	**99.80**	4.36	103.35
16	13.71	0.28	18.90	bdl	0.17	bdl	35.14	6.13	2.67	22.15	**99.15**	4.20	107.76
Aver.	*13.41*	*0.31*	*19.18*	*0.01*	*0.09*	*0.01*	*35.63*	*5.30*	*2.62*	*22.93*	*99.50*	*4.17*	*107.07*

Table V. Results of the electron microprobe analysis of roshchinite grains from Meleg Hill in weight percent (wt%) together with the calculated andorite homologue number (N) and substitution value (L%) (bdl = below the detection limit; No.: measurement ID)

V. táblázat. A meleg-hegyi roscsinitkristályok elektronmikroszondás mérési eredményei tömegszázalékban (wt%), valamint a számított andorithomológ értékek (N) és a helyettesítési százalékok (L%) (bdl = kimutatási határérték alatt; No.: a mérés sorszáma)

No.	Ag	Cu	Pb	Fe	Hg	Zn	Sb	Bi	As	S	Total	N	L%
17	13.88	0.31	15.60	0.03	bdl	bdl	35.31	8.66	3.28	22.26	**99.31**	3.83	120.57
18	13.68	0.25	15.74	bdl	0.11	0.02	35.62	8.26	3.16	22.85	**99.69**	3.78	120.74
19	13.34	0.49	15.79	bdl	0.22	bdl	35.79	8.73	3.32	22.97	**100.65**	3.56	121.79
20	13.83	0.41	15.85	bdl	bdl	bdl	35.28	8.55	3.37	22.67	**99.96**	3.85	119.52
21	13.72	0.29	15.91	0.01	bdl	bdl	35.36	8.76	3.25	22.68	**99.98**	3.76	120.70
22	13.54	0.07	15.84	bdl	0.01	0.07	35.33	8.70	3.29	22.36	**99.21**	3.57	122.77
23	13.68	0.33	15.93	bdl	bdl	0.01	35.93	8.30	3.27	22.56	**100.01**	3.77	121.20
24	13.57	0.00	15.96	0.02	0.14	bdl	35.65	8.30	3.33	22.59	**99.56**	3.62	123.48
25	13.65	0.09	15.95	0.02	bdl	0.07	35.65	8.05	3.36	22.61	**99.45**	3.60	121.94
Aver.	*13.65*	*0.25*	*15.84*	*0.01*	*0.05*	*0.02*	*35.55*	*8.48*	*3.29*	*22.62*	*99.76*	*3.70*	*121.41*

Table VI. Formula coefficients (apfu) of the andorite VI normalized to six sulphur atoms, calculated from the data listed in Table IV (Ado VI: ideal formula of andorite VI; bdl = below the detection limit)

VI. táblázat. *Az andorit VI kristályok 6 kénatomra normált összetétele (apfu) a IV. táblázatban közölt adatok alapján. (Ado VI: az andorit VI ideális formulája; bdl = kimutatási határérték alatt)*

No.	Ag	Cu	ΣMe^{1+}	Pb	Fe	Hg	Zn	ΣMe^{2+}	Sb	Bi	As	ΣMe^{3+}	S
Ado VI			*1*					*1*				*3*	*6*
1	1.05	0.06	**1.10**	0.76	0.01	bdl	0.01	**0.78**	2.58	0.28	0.17	**3.03**	6.09
2	1.09	0.05	**1.14**	0.74	bdl	bdl	0.01	**0.75**	2.55	0.30	0.19	**3.04**	6.07
3	1.06	0.03	**1.08**	0.86	bdl	0.01	bdl	**0.87**	2.68	0.15	0.29	**3.12**	5.93
4	1.11	0.04	**1.16**	0.76	bdl	0.01	bdl	**0.76**	2.61	0.20	0.28	**3.08**	6.00
5	1.03	0.03	**1.06**	0.84	bdl	0.01	bdl	**0.84**	2.60	0.15	0.28	**3.03**	6.07
6	1.11	0.04	**1.15**	0.74	bdl	0.01	bdl	**0.74**	2.51	0.20	0.27	**2.98**	6.13
7	1.11	0.04	**1.15**	0.74	bdl	bdl	bdl	**0.74**	2.46	0.11	0.46	**3.03**	6.08
8	1.06	0.02	**1.09**	0.74	bdl	0.01	bdl	**0.75**	2.26	0.35	0.30	**2.91**	6.26
9	1.03	0.01	**1.04**	0.79	bdl	bdl	bdl	**0.79**	2.36	0.26	0.30	**2.92**	6.25
10	1.04	0.07	**1.11**	0.84	bdl	bdl	bdl	**0.84**	2.38	0.21	0.32	**2.90**	6.15
11	1.01	0.07	**1.08**	0.84	bdl	0.01	bdl	**0.85**	2.41	0.21	0.30	**2.92**	6.15
12	1.01	0.04	**1.05**	0.82	bdl	bdl	bdl	**0.82**	2.45	0.20	0.30	**2.95**	6.19
13	1.01	0.04	**1.05**	0.85	0.01	bdl	bdl	**0.86**	2.47	0.17	0.34	**2.99**	6.10
14	1.03	0.05	**1.08**	0.83	bdl	bdl	bdl	**0.83**	2.48	0.17	0.35	**3.00**	6.09
15	1.12	0.02	**1.15**	0.86	bdl	bdl	bdl	**0.86**	2.47	0.24	0.31	**3.02**	5.97
16	1.10	0.04	**1.14**	0.79	bdl	0.01	bdl	**0.80**	2.50	0.25	0.31	**3.07**	5.99
Aver.	*1.06*	*0.04*	*1.10*	*0.80*	*bdl*	*bdl*	*bdl*	*0.81*	*2.49*	*0.22*	*0.30*	*3.00*	*6.10*

Table VII. Formula coefficients (apfu) of roshchinite measurements normalized to 96 sulphur atoms, calculated from the data listed in Table V (Rch.: ideal formula of roshchinite; bdl = below the detection limit)

VII. táblázat. *A roscsinitkristályok 96 kénatomra normált összetétele (apfu) az V. táblázatban közölt adatok alapján. (Rch: a roscsinit ideális képlete; bdl = kimutatási határérték alatt)*

No.	Ag	Cu	ΣMe^{1+}	Pb	Fe	Hg	Zn	ΣMe^{2+}	Sb	Bi	As	ΣMe^{3+}	S
Rch.			*19*					*10*				*51*	*96*
17	17.79	0.67	**18.46**	10.41	0.07	bdl	0.01	**10.49**	40.10	5.73	6.05	**51.88**	**96**
18	17.08	0.53	**17.61**	10.23	bdl	0.08	0.04	**10.35**	39.40	5.32	5.68	**50.41**	**96**
19	16.57	1.03	**17.60**	10.21	bdl	0.15	bdl	**10.36**	39.38	5.60	5.94	**50.92**	**96**
20	17.41	0.88	**18.28**	10.39	bdl	bdl	bdl	**10.39**	39.34	5.55	6.11	**51.00**	**96**
21	17.26	0.62	**17.88**	10.42	0.02	bdl	bdl	**10.44**	39.41	5.69	5.89	**50.98**	**96**
22	17.28	0.15	**17.43**	10.52	bdl	0.01	0.15	**10.68**	39.94	5.73	6.04	**51.71**	**96**
23	17.30	0.71	**18.01**	10.49	bdl	bdl	0.02	**10.51**	40.26	5.42	5.95	**51.63**	**96**
24	17.14	bdl	**17.14**	10.49	0.05	0.10	bdl	**10.64**	39.89	5.41	6.06	**51.36**	**96**
25	17.23	0.19	**17.42**	10.48	0.05	bdl	0.15	**10.67**	39.85	5.24	6.10	**51.20**	**96**
Aver.	*17.23*	*0.53*	*17.76*	*10.40*	*0.02*	*0.04*	*0.04*	*10.50*	*39.73*	*5.52*	*5.98*	*51.23*	*96*

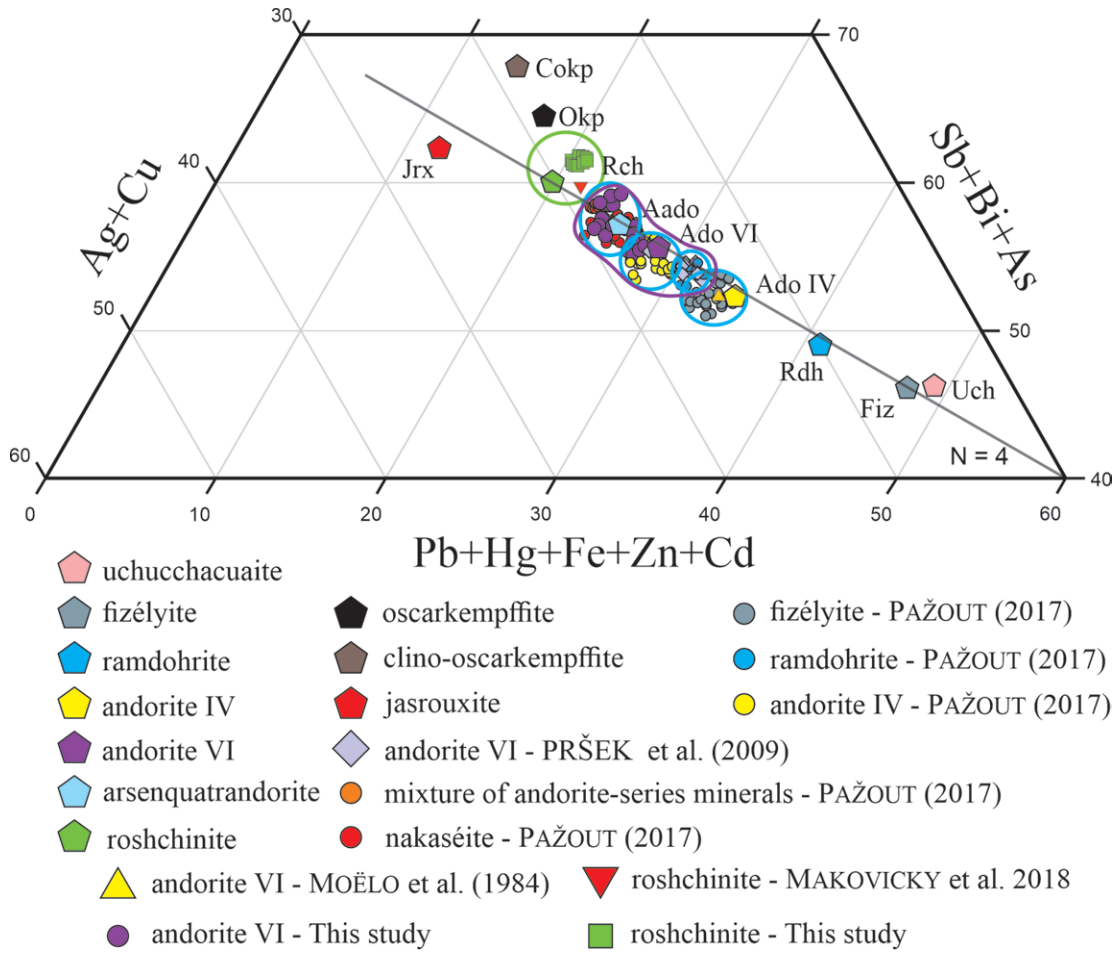

Figure 3. Ternary diagram of the $(Ag_2S + Cu_2S)$-$(Sb_2S_3 + Bi_2S_3 + As_2S_3)$-(PbS + HgS + FeS + ZnS + CdS) showing the andorite substitution $(Ag,Cu)^{+} + (Sb,Bi,As)^{3+} \leftrightarrow 2\ (Pb,Hg,Fe,Zn,Cd)^{2+}$ (andorite series) in 58 measurements from this work and from other authors based on PAŽOUT (2017).

Pentagons: members of the andorite-series minerals with ideal chemical composition; Encircled in blue: field of the andorite-series minerals based on the results of PAŽOUT (2017); Encircled in green: field of roshchinite (Rch) based on results of this study and MAKOVICKY et al. (2018); Encircled in purple: field of andorite VI based on the results of this study and PRŠEK et al. (2009); – N: andorite homologue value; Jrx: jasrouxite, Cokp: clino-oscarkempffite, Okp. oscarkempffite, Rch: roshchinite, Aado: arsenquatrandorite Ado VI: andorite VI, Ado IV: andorite IV, Rdh: ramdohrite, Fiz: fizélyite, Uch: uchucchacuaite; mineral symbols after WARR (2021)

3. ábra. *A meleg-hegyi mintákban azonosított andoritsorbeli ásványok $(Ag_2S + Cu_2S)$-$(Sb_2S_3 + Bi_2S_3 + As_2S_3)$-(PbS + HgS + FeS + ZnS + CdS) háromszögdiagramja (PAŽOUT 2017 nyomán), amely az andorit helyettesítési értéket $(Ag,Cu)^{+} + (Sb,Bi,As)^{3+} \leftrightarrow 2\ (Pb,Hg,Fe,Zn,Cd)^{2+}$ mutatja be a jelen munka 58 mérése, valamint más szerzők eredményei alapján.*

Ötszögek: az andoritsor ideális kémiai összetételű ásványai; Kék körvonallal: az andoritsor ásványainak mezeje PAŽOUT (2017) eredményei alapján; Zöld körvonallal: a roscsinit (Rch) ásvány mezeje jelen munka, valamint MAKOVICKY et al. (2018) eredményei alapján. Lila körvonallal: az andorit VI ásvány mezeje jelen vizsgálat és PRŠEK et al. (2009) alapján; – N: andorithomológ érték; Jrx: jasrouxit, Cokp: klinooscarkempffit, Okp: oscarkempffit, Rch: roscsinit, Aado: arzénkvatrandorit, Ado VI: andorit VI, Ado IV: andorit IV, Rdh: ramdohrit, Fiz: fizélyit, Uch: uchucchacuait; ásványnév-rövidítések és szimbólumok WARR (2021) után

position of roshchinite from Meleg Hill is similar to the sample studied by MAKOVICKY et al. (2018) and to the ideal chemical composition of the species. The chemical composition of roshchinite defines a well distinguishable range on both of the diagrams (*Figure 3*, encircled in green; *Figure 4*, green band). *Figure 4* also shows a well-defined range of andorite VI (purple band) that includes the results of this study, PRŠEK et al. (2009), PAŽOUT (2017) and the ideal andorite VI. In *Figure 3* andorite VI group (purple circle) overlap with the ideal arsenquatrandorite and with the andorite IV and fizélyite measurements of PAŽOUT (2017). The original results of PAŽOUT (2017) show four separate groups of the andorite VI, andorite IV, ramdohrite and fizélyite (*Figure 3*, encircled in blue).

In the case of the samples of PRŠEK et al. (2009) the difference between the ideal positions of the andorite-series minerals and the measured data on the ternary diagram is caused by the Bi-As substitution and the low Me^{2+} content of the samples.

The occurrence of the andorite VI and roshchinite in the north-eastern part of the hydrothermal breccia of Meleg Hill suggests a lower crystallization temperature than that of the enargite-bearing siliceous alterations at the middle and western parts as suggested by the different element enrichments (*cf.* ROBB 2005, OZDÍN & SEJKORA 2009, PRŠEK et al. 2009).

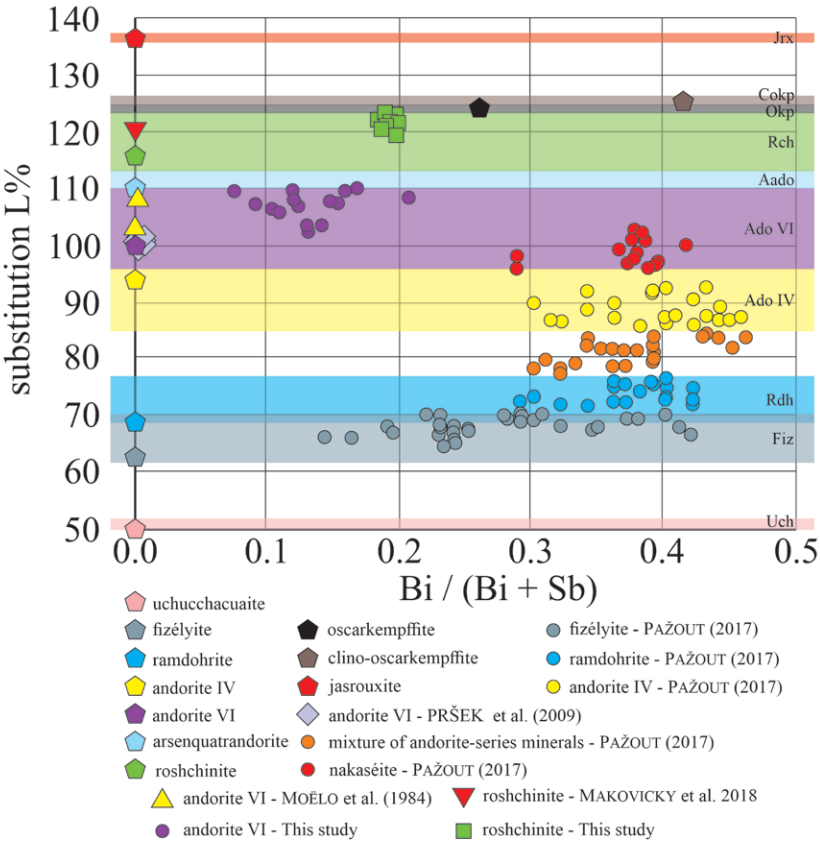

Figure 4. The Bi / (Bi + Sb) (at%) vs. andorite substitution $(Ag,Cu)^{+} + (Sb,Bi,As)^{3+} \leftrightarrow 2\ (Pb,Hg,Fe,Zn,Cd)^{2+}$ plot of andorite-series minerals with 58 measurements from this work and from other authors based on PAŽOUT (2017). The plot shows the ideal (andorite VI), the undersubstituted (uchucchacuaite, fizélyite, ramdohrite and andorite IV) and oversubstituted (arsenquatrandorite, roshchinite, oscarkempffite, clino-oscarkempffite and jasrouxite) members of the andorite series with pentagons. The colour bands represent the fields of the species

Jrx: jasrouxite, Cokp: clino-oscarkempffite, Okp: oscarkempffite, Rch: roshchinite, Aado: arsenquatrandorite Ado VI: andorite VI, Ado IV: andorite IV, Rdh: ramdohrite, Fiz: fizélyite, Uch: uchucchacuaite; mineral symbols after WARR (2021)

4. ábra. *A Bi / (Bi + Sb) (at%) és az andorit helyettesítési százalék $(Ag,Cu)^{+} + (Sb,Bi,As)^{3+} \leftrightarrow 2\ (Pb,Hg,Fe,Zn,Cd)^{2+}$ diagramja (PAŽOUT, 2017 nyomán) a jelen munka 58 mérése, valamint más szerzők eredményei alapján. Az ábrán ötszögekkel jelölve látható az andoritsor ásványainak ideális (andorit VI), alulhelyettesített (uchucchacuait, fizélyit, ramdohrit és andorit IV), valamint túlhelyettesített (arzénkvatrandorit, roscsinit, oscarkempffit, klinooscarkempffit and jasrouxit) tagjai*

Jrx: jasrouxit, Cokp: klinooscarkempffit, Okp: oscarkempffit, Rch: roscsinit, Aado: arzénkvatrandorit, Ado VI: andorit VI, Ado IV: andorit IV, Rdh: ramdohrit, Fiz: fizélyit, Uch: uchucchacuait; ásványnév-rövidítések WARR (2021) után

Conclusions

With SEM imaging and EPMA measurements, two different andorite-series minerals were observed at Meleg Hill, Velence Mts., Hungary: andorite VI and roshchinite. Both occur in the silicious matrix and the crystals are intergrown with each other. The andorite-series minerals have a flame-like or fibrous appearance. Individual crystals vary in size. The fibrous form is usually less than 1 μm in width and the length of the flame-like variety is between 1–50 μm.

Individual grains were analysed to determine their exact chemical composition. From the obtained data the andorite homologue value (N) and the substitution percentage (L%) were calculated to determine the position of the minerals within the andorite series. The chemical formula of the minerals are as follows:

Andorite VI (L% = 102.65–109.84) (N = 3.99–4.41) with $Ag_{1.01–1.12}Cu_{0–0.07}Pb_{0.74–0.86}Zn_{0–0.01}Hg_{0–0.01}Fe_{0–0.01}Sb_{2.26–2.68}Bi_{0.11–0.35}As_{0.11–0.46}S_6$ and roshchinite (L% = 119.52–123.48) (N = 3.56–3.85) with $Ag_{16.68–17.71}Cu_{0–1.04}Pb_{10.28–10.55}Zn_{0–0.15}Hg_{0–0.15}Fe_{0–0.07}Sb_{39.41–40.22}Bi_{5.26–5.74}As_{5.734–6.13}S_{96}$.

The formerly used comparative ternary diagrams of the system $(Ag_2S + Cu_2S)–(Sb_2S_3 + Bi_2S_3 + As_2S_3)–(PbS + HgS + FeS + ZnS + CdS)$ and the Bi / (Bi + Sb) (at%) vs. andorite substitution $(Ag,Cu)^{+} + (Sb,Bi,As)^{3+} \leftrightarrow 2\ (Pb,Hg,Fe,Zn,Cd)^{2+}$ plot of andorite-series minerals are not adequate enough to separate the species from each other due to the highly variable element substitution in the case of Me^{+}, Me^{2+} and Me^{3+} cations.

Calculation of the andorite substitution percentage (L%) and the homologue order value (N), with their combined representation on the two diagrams is always necessary to distinguish the mineral species.

Andorite VI and roshchinite were identified in Hungary for the first time.

Acknowledgements

The authors are grateful for the access to the investigated sample granted by the Department of Mineralogy, Herman Ottó Museum, Miskolc, Hungary.

The research was carried out at the University of Miskolc both as part of the „More efficient exploitation and use of subsurface resources” project implemented in the framework of the Thematic Excellence Program funded by the Ministry of Innovation and Technology of Hungary (Grant Contract reg. nr.: NKFIH-846-8/2019) and the “Developments aimed at increasing social benefits deriving from more efficient exploitation and utilization of domestic subsurface natural resources” project supported by the Ministry of Innovation and Technology of Hungary from the National Research, Development and Innovation Fund in line with the Grant Contract issued by the National Research, Development and Innovation Office (Grant Contract reg. nr.: TKP-17-1/PALY-2020).

Special thanks to our reviewers, Gábor PAPP (Hungarian Natural History Museum, Budapest) and Zsolt BENKÓ (Institute for Nuclear Research, Debrecen) for their valuable contribution to improving the quality of the manuscript.

References – Irodalom

Bajnóczi, B., Molnár, F., Maeda, K., Nagy, G. & Vennemann, T. 2010: Mineralogy and genesis of primary alunites from epithermal systems of Hungary. – *Acta Geologica Hungarica* **45/1,** 101–118. https://doi.org/10.1556/ageol.45.2002.1.6

Balla, Z. 1985: The Carpathian loop and the Pannonian basin: a kinematic analysis. – *Geophysical Transactions* **30/4,** 313–353.

Benedek K., Pécskay, Z., Szabó, Cs., Jósfai, J. & Németh, T. 2004: Palaeogene igneous rocks in the Zala basin (Western Hungary): link to the Palaeogene magmatic activity along the Periadriatic lineament. – *Geologica Carpathica* **55/1,** 43–50. https://doi.org/10.1556/ageol.45.2002.4.3

Benkó, Z., Molnár, F. & Lespinasse, M. 2008: Application of studies on fluid inclusion planes and fracture systems in the reconstruction of the fracturing history of granitoid rocks I: Introduction to methods and implications for fluid-mobilisation events in the Velence Hills. – *Bulletin of the Hungarian Geological Society* **138/3,** 229–246. (In Hungarian)

Benkó, Zs., Molnár, F., Lespinasse, M., Billström, K., Pécskay, Z. & Németh, T. 2010: Genetic and age relationship of the base metal mineralization along the Periadriatic–Balaton Lineament system on the basis of radiogenic isotope studies. – *Acta Mineralogica-Petrographica Abstract Series (IMA2010 Conference, Budapest)* **6,** p. 224.

Benkó, Z., Molnár, F., Pécskay, Z. & Németh, T. 2012: The interplay of the Paleogene magmatic-hydrothermal fluid flow on a Variscan granite intrusion: age and formation of the barite vein at Sukoró, Velence Mts, W-Hungary. – *Bulletin of the Hungarian Geological Society* **142/1,** 45–85. (In Hungarian)

Benkó, Zs., Molnár, F., Billström, K. & Pécskay, Z. 2014: Triassic fluid mobilization and epigenetic lead-zinc sulphide mineralization in the Transdanubian Shear Zone (Pannonian Basin, Hungary). – *Geologica Carpathica* **65/3,** 177–194. https://doi.org/10.2478/-geoca-2014-0012

Buda, Gy. 1993: Enclaves and fayalite-bearing pegmatitic "nests" in the upper part of the granite intrusion of the Velence Mts., Hungary. – *Geologica Carpathica* **44,** 143–153.

Buda, Gy., Koller, F. & Ulrych, J. 2004: Petrochemistry of Variscan granitoids of Central Europe: Correlation of Variscan granitoids of the Tisia and Pelsonia Terranes with granitoids of the Moldanubicum, Western Carpathian and Southern Alps. A review: Part I. – *Acta Geologica Hungarica* **47,** 117–138. https://doi.org/10.1556/ageol.47.2004.2-3.3

Csontos, L. & Vörös, A. 2004: Mesozoic plate tectonic reconstruction of the Carpathian region. – *Palaeogeography, Palaeoclimatology, Palaeoecology* **210/1,** 1–56. https://doi.org/10.1016/j.palaeo.2004.02.033

Darida-Tichy, M. 1987: Paleogene andesite volcanism and associated rock alteration (Velence Mountains, Hungary). – *Geologica Carpathica* **38/1,** 19–34.

Gyalog, L. 2005a: *Geological map of Hungary. L-34-25 Székesfehérvár. 1:100,000.* – Geological Institute of Hungary, Budapest

Gyalog, L. 2005b: *Geological map of Hungary. L-34-26 Százhalombatta (Ráckeve). 1:100,000.* – Geological Institute of Hungary, Budapest

Gyalog, L. & Horváth, I. 2004: *Geology of the Velence Hills and the Balatonfő.* – Geological Institute of Hungary, Budapest, 316 p.

Horváth, I., Darida-Tichy, M., Dudko, A., Gyalog, L. & Ódor, L. 2004: *Geology of the Velence Hills and the Balatonfő. Explanatory Book of the Geological Map of the Velence Hills (1:25 000).* – Geological Institute of Hungary, Budapest, 253–316.

Jantsky, B. A. 1957: Geology of the Velence Mountains. – *Geologica Hungarica. Series Geologica* **10,** 1–170. (In Hungarian)

Kázmér, M. & Kovács, S. 1985: Permian–Paleogene paleogeography along the eastern part of the Insubric–Periadriatic lineament system: Evidence for continental escape of the Bakony–Drauzug Unit. – *Acta Geologica Hungarica* **28/1–2,** 71–84.

Kostov, I. & Minčeva-Stefanova, J. 1981: *Sulphide Minerals - Crystal chemistry, parageneses and systematics* – The Bulgarian Academy of Sciences, Sofia, Bulgaria, 211 p.

Kovács, I., Németh, T., B. Kiss, G., K. Kis V., Tóth, Á. & Benkó, Zs. 2019: Rare aluminium phosphates and sulphates (APS) and clay mineral assemblages in silicified hydraulic breccia hosted by a Permian granite (Velence Mts., Hungary) as indicators of a high sulfidation type epithermal system. – *Mineralogy and Petrology* **113**, 217–228. https://doi.org/10.1007/s00710-018-0644-1

Kovács, I., Németh, T., B. Kiss, G. & Benkó, Zs. 2020: Application of the capillary method in micro X-ray diffractometry (μ-XRD): A useful technique for the characterization of small amounts of clay minerals. – *Central European Geology* **64/1,** 1–7. https://doi.org/10.1556/24.2020.00005

Makovicky, E. 2019: Algorithms for calculations of homologue order N in the homologous series of sulfosalts. – *European Journal of Mineralogy* **31,** 83–97. https://doi.org/10.1127/ejm/2018/0030-2791

Makovicky, E. & Karup-Møller, S. 1977a: Chemistry and crystallography of the lillianite homologous series. Part I. General properties and definitions. – *Neues Jahrbuch für Mineralogie, Abhandlungen* **130/3,** 264–287.

Makovicky, E. & Karup-Møller, S. 1977b: Chemistry and crystallography of the lillianite homologous series. Part II: Definition of new minerals: eskimoite, vikingite, ourayite, and treasurite. Redefinition of schirmerite and new data on the lillianite-gustavite solid solution series. – *Neues Jahrbuch für Mineralogie, Abhandlungen* **131,** 56–82.

Makovicky, E. & Mumme, W. G. 1983: The crystal structure of ramdohrite, $Pb_6Sb_{11}Ag_3S_{24}$, and its implications for the andorite group and zinckenite. – *Neues Jahrbuch für Mineralogie, Abhandlungen* **147/1,** 58–79.

Makovicky, E., Mumme, W. G. & Gable, R. W. 2013: The crystal structure of ramdohrite, $Pb_{5.9}Fe_{0.1}Mn_{0.1}In_{0.1}Cd_{0.2}Ag_{2.8}Sb_{10.8}S_{24}$: A new refinement. – *American Mineralogist* **98/4,** 773–779. https://doi.org/10.2138/am.2013.4146

Makovicky, E., Stöger, B. & Topa, D. 2018: The incommensurately modulated crystal structure of roshchinite, $Cu_{0.09}Ag_{1.04}Pb_{0.65}Sb_{2.82}As_{0.37}S_{6.08}$. – *Zeitschrift für Kristallographie – Crystalline Materials* **233/3–4,** 255–267. https://doi.org/10.1515/zkri-2017-2126

Moëlo, Y., Makovicky, E. & Karup-Møller, S. 1984: New data on minerals of the andorite series. – *Neues Jahrbuch für Mineralogie, Monatshefte* **1984/4,** 175–182.

Moëlo, Y., Makovicky, E., Mozgova, N. N., Jambor, J. L., Cook, N., Pring, A., Paar, W., Nickel, E. H., Graeser, S., Kraup-Møller, S., Balic-Žunic, T., Mumme, W. G., Vurro, F., Topa, D., Bindi, L., Bente, K. & Shimizu, M. 2008: Sulfosalt systematics: a review. Report of the sulfosalt sub-committee of the IMA Commission on Ore Mineralogy. – *European Journal of Mineralogy* **20,** 7–46. https://doi.org/10.1127/0935-1221/2008/0020-1778

Molnár, F. 1996: Fluid inclusion characteristics of Variscan and alpine metallogeny of the Velence Mts., W-Hungary. – *Plate Tectonic Aspects of the Alpine Metallogeny in the Carpatho-Balkan Region, Proceedings of the Annual Meeting-Sofia, UNESCO-IGCP Project No 3* **56/2,** 29–44.

Molnár, F. 1997: Contributions to the genesis of molybdenite in the Velence Mts.: mineralogical and fluid inclusion studies on the mineralization of the Retezi adit. – *Bulletin of the Hungarian Geological Society* **127/1–2,** 1–17. (In Hungarian)

Molnár, F. 2004: Characteristics of Variscan and Palaeogene fluid mobilization and ore forming processes in the Velence Mts., Hungary: a comparative fluid inclusion study. – *Acta Mineralogica-Petrographica* **45/1,** 55–63.

Molnár, F., Török, K. & Jones, P. 1995: Crystallization conditions of pegmatites from the Velence Mts., Western Hungary, on the basis of thermobarometric studies. – *Acta Geologica Hungarica* **38/1,** 57–80.

Molnár F., Bajnóczi B., Pécskay Z., Prohászka A. & Benkó Zs. 2010: Hydrothermal alteration, fluid inclusions and stable isotopes (O, H) in a porphyry and related epithermal system of the Palaeogene volcanic belt of the Alp-Carpathian Orogen (Velence Mts., W-Hungary). – *Acta Mineralogica-Petrographica Abstract Series (IMA2010 Conference, Budapest)* **6,** p. 289.

Ozdín, D. & Sejkora, J. 2009: Andorite IV and andorite VI from the Dúbrava deposit in the Nízke Tatry Mts. (Slovak Republic). – *Bulletin mineralogicko-petrologického oddělení Národního muzea v Praze* **17/1,** 65–68. (In Czech)

Pažout, R. 2017: Lillianite homologues from Kutná Hora ore district, Czech Republic: A case of large-scale Sb for Bi substitution. – *Journal of Geosciences* **62,** 37–57. https://doi.org/10.3190/jgeosci.235

Pršek, J., Lauko, L. & Valášková, M. 2009: Andorite VI from stibnite mineralization in the Spiš-Gemer Ore Mts. (Zlatá Idka, Dobšiná-Tiefengründel localities). – *Mineralia Slovaca* **41,** 183–190.

Robb, L. 2005: *Introduction to ore forming processes.* – Blackwell Science, Malden, 373 p.

Topa, D., Makovicky, E., Favreau, G., Bourgoin, V., Boulliard, J., Zagler, G. & Putz, H. 2013: Jasrouxite, a new Pb–Ag–As–Sb member of the lillianite homologous series from Jas Roux, Hautes-Alpes, France. – *European Journal of Mineralogy* **25,** 1031–1038. https://doi.org/10.1127/0935-1221/2013/0025-2336

Tóth, Á. 2016: Investigation of hydrothermal breccia from Meleg Hill. – *MSc Thesis*, Eötvös Loránd University, Budapest (In Hungarian)

Uher, P. & Broska, I. 1994: The Velence Mts granitic rocks: geochemistry, mineralogy and comparison to Variscan Western Carpathian granitoids. – *Acta Geologica Hungarica* **37/1–2,** 45–66.

Warr, N. L. 2021: IMA–CNMNC approved mineral symbols. – *Mineralogical Magazine* **85/3,** 291–320. https://doi.org/10.1180/mgm.2021.43

Manuscript recieved: 15/03/2022